

Interpretation of Experimental J^{PC} Exotic Signals

Alexander Donnachie* and Philip R. Page†

*Theory Group, Thomas Jefferson National Accelerator Facility,
12000 Jefferson Avenue, Newport News, VA 23606, USA*

June 1998

Abstract

We investigate theoretical interpretations of the 1.4 GeV J^{PC} exotic resonance reported by the E852 collaboration. It is argued that interpretation in terms of a hybrid meson is untenable. A K-matrix analysis shows that the 1.4 GeV enhancement in the E852 $\eta\pi$ data can be understood as an interference of a non-resonant Deck-type background and a resonance at 1.6 GeV. A final state rescattering calculation shows that the 1.6 GeV hybrid has a $\eta\pi$ width which is bounded above by 57 ± 14 MeV.

Keywords: exotic, hybrid meson, K-matrix, Deck background, doorway

PACS number(s): 12.39.Mk 12.40.Nn 13.25.Jx 13.75.Gx 14.40.Cs

**E-mail: ad@a3.ph.man.ac.uk. Current address: Department of Physics and Astronomy, University of Manchester, Manchester M13 9PL, UK.*

†*E-mail: prp@t5.lanl.gov. Current address: T-5, MS-B283, Los Alamos National Laboratory, P.O. Box 1663, Los Alamos, NM 87545, USA.*

1 Introduction

Evidence for a $J^{PC} = 1^{-+}$ isovector resonance $\hat{\rho}(1405)$ at 1.4 GeV in the reaction $\pi^- p \rightarrow \eta\pi^- p$ has been published recently by the E852 collaboration at BNL [1]. The mass and width quoted are $1370 \pm 16_{-30}^{+50}$ MeV and $385 \pm 40_{-105}^{+65}$ respectively. These conclusions are strengthened by the claim of the Crystal Barrel collaboration that there is evidence for the same resonance in $p\bar{p}$ annihilation with a mass of $1400 \pm 20 \pm 20$ MeV and a width of $310 \pm 50_{-30}^{+50}$ MeV [2], consistent with E852. However, the Crystal Barrel state is not seen as a peak in the $\eta\pi$ mass distribution, but is deduced from interference in the Dalitz plot. Since the J^{PC} of this state is “exotic”, i.e. it implies that it is *not* a conventional meson, considerable excitement has been generated, particularly because the properties of the state appear to be in conflict with theoretical expectations. The resonance is reported in natural parity exchange in the E852 experiment, and no statement can currently be made about its production in unnatural parity exchange.

In addition there are two independent indications of a more massive isovector $J^{PC} = 1^{-+}$ exotic resonance $\hat{\rho}(1600)$ in $\pi^- N \rightarrow \pi^+\pi^-\pi^- N$. The E852 collaboration recently reported evidence for a resonance at $1593 \pm 8_{-47}^{+29}$ MeV with a width of $168 \pm 20_{-12}^{+150}$ MeV [3]. These parameters are consistent with the preliminary claim by the VES collaboration of a resonance at 1.62 ± 0.02 GeV with a width of 0.24 ± 0.05 GeV [4]. In both cases a partial wave analysis was performed, and the decay mode $\rho^0\pi^-$ was observed. There is also evidence for $\hat{\rho}(1600)$ in $\eta'\pi$ peaking at 1.6 GeV [5]. It has been argued that the $\rho\pi$, $\eta'\pi$ and $\eta\pi$ couplings of this state qualitatively support the hypothesis that it is a hybrid meson, although other interpretations cannot be entirely eliminated [6].

Recent flux-tube and other model estimates [7] and lattice gauge theory calculations [8] for the lightest 1^{-+} hybrid support a mass substantially higher than 1.4 GeV and often above 1.6 GeV [6]. Further, on quite general grounds, it can be shown that an $\eta\pi$ decay of 1^{-+} hybrids is unlikely [9]. There is thus an apparent conflict between experimental observation and theoretical expectation as far as the 1.4 GeV peak is concerned.

The purpose of the present paper is to propose a resolution of this apparent conflict. Two possible hypotheses are considered.

1. The two states are indeed separate resonances and are hybrid mesons: the lower one the ground state and the upper one an excited state. We perform calculations in the

flux-tube model of Isgur and Paton [10] to demonstrate that both on mass and decay grounds, this hypothesis is implausible.

2. We suggest a mechanism whereby an appropriate $\eta\pi$ decay of a hybrid meson can be generated and argue that there is only one $J^{PC} = 1^{-+}$ isovector exotic, the lower-mass signal in the E852 experiment being an artefact of the production dynamics. We demonstrate explicitly that it is possible to understand the 1.4 GeV peak observed in $\eta\pi$ as a consequence of a 1.6 GeV resonance interfering with a non-resonant Deck-type background with an appropriate relative phase. We do *not* propose that there should necessarily be a peak at 1.4 GeV; but that if experiment unambiguously confirms a peak at 1.4 GeV, it can be understood as a 1.6 GeV resonance interfering with a non-resonant background.

2 Hypothesis I: Two hybrid mesons close in mass

The simplest explanation for the experimental report of two peaks at two different masses, is that they are indeed separate Breit-Wigner resonances.

The most conservative assumption is that these are then both hybrid mesons. Other less likely hypotheses, such as glueball, four-quark and molecular interpretations, are discussed in ref. [6].

In the hybrid scenario, the 1.4 GeV resonance would naturally be assumed to be the ground state hybrid and the 1.6 GeV resonance an excited hybrid. A numerical calculation in the flux-tube model indicates that the orbitally excited D-wave hybrid is the lowest excitation above the P-wave ground state, with a mass difference of 400 MeV for light quarks [7]. The same model predicts $c\bar{c}$ D-wave hybrids to be 270 MeV heavier than the ground state hybrid [7], in good agreement with the result of 230 MeV found in adiabatic-limit lattice-gauge theory simulations [8] and similar results in NRQCD lattice simulations [11]. Also, the lattice-gauge calculations find that the next highest levels in the $c\bar{c}$ sector are the radially excited P-wave hybrids [11], which are 400 MeV heavier than the ground state [8]. A mass difference of 400 MeV for the light-quark hybrids is clearly inconsistent with the experimental claim of resonances at 1.4 and 1.6 GeV. The absolute mass scale predicted by

Table 1: Decay widths of a ground state at 1.4 GeV in the flux-tube model. The $f_2\pi$, $\rho\omega$, K^*K , $\eta\pi$ and $\eta'\pi$ modes are all substantially below 1 MeV. The conventions and parameters are those of ref. [13], except for the following changes for the $b_1\pi$ and $f_1\pi$ modes. Here we use a radial dependence of the hybrid $\sim r$, which produces widths $\sim 5\%$ different from ref. [13]. More importantly, we take into account the fact that the b_1 and f_1 have finite widths, and we assume that they decay predominantly to $\omega\pi$ and $a_0(980)\pi$ respectively.

Decay Mode	Partial Wave	Width (MeV)
$b_1\pi$	S,D	96
$f_1\pi$	S,D	13
$\rho\pi$	P	4
$\eta(1295)\pi$	P	< 1

theory does not¹ support a ground state hybrid at 1.4 GeV, as discussed in ref. [6]. Thus there are two arguments on mass grounds for discarding this hypothesis.

Further, from the viewpoint of decays, it is qualitatively hard to explain why the lower-mass 1^{-+} hybrids should be seen only in $\eta\pi$. This is because relativistic symmetrization selection rules suppress the $\eta\pi$ decay of *any* 1^{-+} hybrid in QCD in the absence of final state interactions [9]. Within the flux-tube model and constituent-gluon models there is a selection rule which suppresses decays of ground state hybrids to two S-wave mesons [13, 14]. This selection rule requires only the standard assumptions of non-relativistically moving quarks and spin 1 pair creation in a connected decay topology [15]. In addition, for 1^{-+} hybrids the selection rule is only operative when the non-relativistic spin of the $Q\bar{Q}$ is 1. The lowest orbitally excited hybrid in the flux-tube model has $Q\bar{Q}$ in spin 1, and hence obeys the selection rule. The ground and lowest excited hybrids have hence got similar overall decay structure.

Flux-tube model predictions for the decay of a 1.4 GeV hybrid are given in Table 1. We note that the total predicted width of ~ 110 MeV is much smaller than the observed value. The calculations show that we expect an appreciably larger $\rho\pi$ width than $\eta\pi$ width for the ground state hybrid. This is confirmed by QCD sum rule calculations [16]. It then

¹Except for a QCD sum rule prediction of ~ 1.5 GeV [12].

Table 2: Decay widths of an orbitally excited hybrid at 1.6 GeV to $P + S$ -wave states in the flux-tube model in MeV. The conventions and parameters are those of ref. [13]. The derivation of the widths is discussed in Appendix A. The inverse radius of the hybrid $\beta_{\hat{\rho}} = 0.27$ GeV is taken to be the same as that of the ground state hybrid [13]. We also quote an error based on taking $\beta_{\hat{\rho}} = 0.23$ GeV. Widths of a 2 GeV orbitally excited hybrid is also indicated for comparison.

Decay Mode	Partial Wave	Excited Hybrid Mass	
		1.6 GeV	2.0 GeV
$b_1\pi$	S	118 (-22)	10 (-5)
	D	.1	.8
$f_1\pi$	S	30 (-5)	4 (-1)
	D	.05	12 (-1)
$f_2\pi$	D	.08	2
$a_1\eta$	S	-	11 (-3)
	D	-	2
$a_2\eta$	S	-	.07
$K_1(1270)K$	S	-	105 (-27)
	D	-	.5
$K_1(1400)K$	S	-	.05
	D	-	.3
$K_2^*(1430)K$	D	-	.03

becomes difficult to understand how there can be almost no presence of 1^{-+} wave in the $\rho\pi$ experimental data at 1.5 GeV [3], where there should be significant presence due to the ~ 400 MeV width of the E852 1.4 GeV state. This calls into question the interpretation of the 1.4 GeV state as a ground state hybrid. When final state interactions are taken into account (a point on which we elaborate below), we expect a larger $\eta\pi$ width, which may invalidate the preceding arguments. We shall hence proceed with the hypothesis that the 1.4 GeV state is the ground state hybrid and the 1.6 GeV state the orbitally excited hybrid. According to the flux-tube model calculations in Table 2, the orbitally excited hybrid at 1.6 GeV has a somewhat larger total width than the the ground state hybrid at 1.4 GeV.

This is a strong theoretical statement as generally nodes in orbital wave functions tend to suppress specific partial widths relative to the ground state. Note that P–wave modes like $\eta(1295)\pi$, K^*K , $\rho\omega$ should all be stronger² for a 1.6 GeV state than a 1.4 GeV state, simply due to phase space. Thus there is a further problem in understanding why the 1.4 GeV state should have a larger experimental width than the 1.6 GeV state.

So on a multiplicity of grounds we are forced to conclude that the hypothesis that the 1.4 and 1.6 GeV states are both hybrid mesons is theoretically untenable.

3 Hypothesis II: A single hybrid meson at 1.6 GeV

The current experimental data on the 1.6 GeV state is consistent with mass predictions and decay calculations for a hybrid meson [6, 17]. This then leaves open the interpretation of the structure at 1.4 GeV.

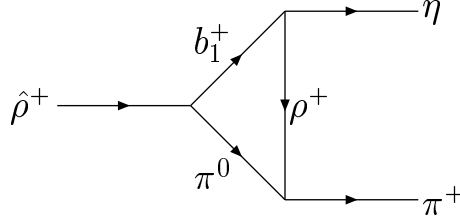
There are two basic problems to be solved. Firstly it is necessary to find a mechanism which can generate a suitable $\eta\pi$ width for the hybrid. Then having established that, it is necessary to provide a mechanism to produce a peak in the cross section which is some way below the real resonance position.

We first show that a sizable $\eta\pi$ width for a hybrid resonance can be generated by final–state interactions. For this we use a doorway calculation, the procedures for which are well established [18]. We use the simplest approach to provide an upper limit.

The $\eta\pi$ peak in the E852 data spans the $\rho\pi$ and $b_1\pi$ thresholds, so we propose a Deck–type model [19] as a source of a non–resonant $\eta\pi$ background. We then show that, within the K–matrix formalism, interference between this background and a resonance at 1.6 GeV can account for the E852 $\eta\pi$ data. The width used for the decay of the 1.6 GeV hybrid to $\eta\pi$ is comfortably below the upper limit established in the doorway calculation.

²In constituent gluon models, the lowest–lying excited hybrid is expected to have $Q\bar{Q}$ spin 0, so that decays to S–wave mesons are not suppressed [14, 15]. The lowest–lying excited hybrid would then be very wide indeed.

Figure 1: Decay of $\hat{\rho}$ to $\eta\pi$ via final state interactions.



3.1 $\eta\pi$ doorway width of a 1.6 GeV state

Although the $\eta\pi$ width of a hybrid is suppressed by symmetrization selection rules [9] which operate on the quark level and have been estimated in QCD sum rules to be tiny (~ 0.3 MeV) [16], long distance contributions to this width are possible. We shall show that these can be very much larger than the widths obtained without final state interactions.

The procedure we adopt is that of a doorway calculation with on-shell mesons [18], which provides an upper limit. An essential ingredient is the presence of an allowed dominant decay which can couple strongly to the channel of interest. In the flux-tube model $b_1\pi$ is such a dominant decay, and it is strongly coupled to $\eta\pi$ by ρ exchange (see Figure 1). So we consider the process $\hat{\rho}^+ \rightarrow b_1\pi \rightarrow \eta\pi^+$.

For on-shell states the Lorentz invariant amplitudes can be parameterized as

$$\mathcal{M}_{\hat{\rho} \rightarrow b_1^+ \pi^0} = \epsilon_\mu^\rho \epsilon_\nu^{b_1^*} (g_{\hat{\rho} b_1 \pi}^S g^{\mu\nu} + g_{\hat{\rho} b_1 \pi}^D p_{b_1}^\mu p_\rho^\nu) \quad (1)$$

$$\mathcal{M}_{b_1 \rightarrow \rho^+ \eta} = \epsilon_\mu^{b_1} \epsilon_\nu^{\rho^*} (g_{b_1 \rho \eta}^S g^{\mu\nu} + g_{b_1 \rho \eta}^D p_\rho^\mu p_{b_1}^\nu) \quad (2)$$

$$\mathcal{M}_{\rho \rightarrow \pi^+ \pi^0} = g_{\rho \pi \pi} \epsilon_\mu^\rho (p_{\pi^+}^\mu - p_{\pi^0}^\mu) \quad (3)$$

where p_X^μ and ϵ_μ^X refer to the momentum and polarization 4-vectors of X respectively, $g^{\mu\nu}$ is the flat space metric tensor, and $g_{\hat{\rho} b_1 \pi}^S$, $g_{\hat{\rho} b_1 \pi}^D$, $g_{b_1 \rho \eta}^S$, $g_{b_1 \rho \eta}^D$ and $g_{\rho \pi \pi}$ are decay constants to be determined. These are discussed in Appendix B.

The doorway amplitude for the process $\hat{\rho} \rightarrow b_1^+ \pi^0 \rightarrow \eta\pi^+$ is then

$$\begin{aligned}
\mathcal{M}_{doorway} &= \frac{i}{(2\pi)^4} \int d^4 p_{b_1} \epsilon_{\hat{\rho}}^{\mu} (g_{\hat{\rho}b_1\pi}^S g^{\mu\nu} + g_{\hat{\rho}b_1\pi}^D p_{b_1}^{\mu} p_{\hat{\rho}}^{\nu}) \frac{g_{\nu\sigma}}{p_{b_1}^2 - m_{b_1}^2 + i\epsilon} \\
&\times (g_{b_1\rho\eta}^S g^{\sigma\lambda} + g_{b_1\rho\eta}^D p_{\rho}^{\sigma} p_{b_1}^{\lambda}) \frac{g_{\lambda\kappa}}{p_{\rho}^2 - m_{\rho}^2 + i\epsilon} g_{\rho\pi\pi} (p_{\pi^+}^{\kappa} - p_{\pi^0}^{\kappa}) \frac{1}{p_{\pi^0}^2 - m_{\pi^0}^2 + i\epsilon}
\end{aligned} \quad (4)$$

where ϵ is a small real number. Here we have contracted the Lorentz indices on the internal vector particles in the usual way [18], effectively working in the ‘‘Feynman gauge’’. Integration is performed over the loop momentum. We evaluate the doorway amplitude in the rest frame of $\hat{\rho}$ using conservation of momentum at the vertices and the Cutkovsky rules to obtain [18]

$$\mathcal{M}_{doorway} = \frac{i g_{\rho\pi\pi}}{32\pi(E_{b_1} + E_{\pi^0})q} \{(\varsigma_1 + \varsigma_2 z + \varsigma_3 z^2) \ln \left| \frac{1+z}{1-z} \right| - 2(\varsigma_2 + z\varsigma_3)\} \quad (5)$$

if the component of the polarization of $\hat{\rho}$ is in the direction of the outgoing particles, i.e. η or π^+ . For other polarizations, $\mathcal{M}_{doorway} = 0$.

Here

$$\varsigma_1 = -g_{\hat{\rho}b_1\pi}^S q \{g_{b_1\rho\eta}^S + g_{b_1\rho\eta}^D (E_{b_1} (E_{\pi^0} + E_{\pi^+}) + p^2)\} \quad (6)$$

$$\begin{aligned}
\varsigma_2 &= p \{-g_{\hat{\rho}b_1\pi}^S g_{b_1\rho\eta}^S + g_{\hat{\rho}b_1\pi}^D g_{b_1\rho\eta}^S m_{\hat{\rho}} (E_{\pi^0} + E_{\pi^+}) + \\
&(g_{\hat{\rho}b_1\pi}^S g_{b_1\rho\eta}^D + g_{\hat{\rho}b_1\pi}^D g_{b_1\rho\eta}^D m_{\hat{\rho}} (E_{b_1} - E_{\eta})) (E_{b_1} (E_{\pi^0} + E_{\pi^+}) + p^2) - g_{\hat{\rho}b_1\pi}^S g_{b_1\rho\eta}^D q^2\}
\end{aligned} \quad (7)$$

$$\varsigma_3 = g_{b_1\rho\eta}^D p^2 q \{g_{\hat{\rho}b_1\pi}^S + g_{\hat{\rho}b_1\pi}^D m_{\hat{\rho}} (E_{b_1} - E_{\eta})\} \quad (8)$$

$$z = \frac{p^2 + q^2 - (E_{b_1} - E_{\eta})^2 + m_{\rho}^2}{2pq} \quad (9)$$

and p is the magnitude of the b_1 or π^0 momentum, q the magnitude of the η or π^+ momentum, and E_X the energy of X , all in the rest frame of $\hat{\rho}$.

The doorway decay width for $\hat{\rho}^+ \rightarrow b_1\pi \rightarrow \eta\pi^+$ is then

$$\Gamma_{\hat{\rho} \rightarrow b_1 \pi \rightarrow \eta \pi^+} = \frac{q}{8\pi m_{\hat{\rho}}^2} \frac{1}{3} |2 \mathcal{M}_{doorway}|^2 \quad (10)$$

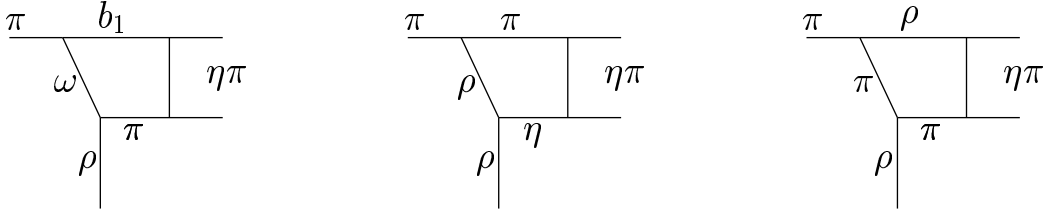
where we have taken into account that there are two possible intermediate processes contributing to the total amplitude, i.e. $\hat{\rho}^+ \rightarrow b_1^+ \pi^0 \rightarrow \eta \pi^+$ and $\hat{\rho}^+ \rightarrow b_1^0 \pi^+ \rightarrow \eta \pi^+$.

We calculate that the doorway width is 57 ± 14 MeV for all the particles on-shell, taking into account uncertainties in the couplings $b_1^+ \rightarrow \rho^+ \eta$ and $\rho^+ \rightarrow \pi^+ \pi^0$ (see Appendix B). As remarked in Appendix B, there are uncertainties in the coupling $\hat{\rho}^+ \rightarrow b_1^+ \pi^0$ which can make this doorway width up to $\sim 40\%$ smaller. Thus we conclude that the doorway width is less than 57 ± 14 MeV. It should also be remembered that the doorway calculation as it stands provides an upper limit, since we would get a smaller answer if we were to take one of the internal legs off-shell and introduce form factors [20]. However these are unknown, and as 57 ± 14 MeV is well above the $\eta\pi$ width required this does not create a problem.

3.2 Non-resonant $\eta\pi$ Deck background

The 1.4 GeV peak in the $\eta\pi$ channel occurs in the vicinity of the $\rho\pi$ and $b_1\pi$ thresholds, and it is therefore natural to consider these as being responsible in some way for the $\eta\pi$ peak. The Deck mechanism [19] is known to produce broad low-mass enhancements for a particle pair in three-particle final states, for example in $\pi p \rightarrow (\rho\pi)p$. In this latter case, the incident pion dissociates into $\rho\pi$, either of which can then scatter off the proton [21]. At sufficiently high energy and presumed dominance of the exchange of vacuum quantum numbers (pomeron exchange) for this scattering one obtains the “natural parity change” sequence $\pi \rightarrow 0^-, 1^+, 2^-, \dots$ (the Gribov–Morrison rule [22]). However if the scattering involves the exchange of other quantum numbers then additional spin-parity combinations can be obtained, including $J^P = 1^-$. This can be seen explicitly in ref. [19] for the reaction $\pi p \rightarrow (\rho\pi)p$ in which the full πp scattering amplitude was used, so that the effect of exchanges other than the pomeron are automatically included. The J^P sequence from the “natural parity change” dominates due to the dominant contribution from pomeron exchange, but other spin-parity states are present at a non-negligible level. The Reggeised Deck effect can simulate resonances, both in terms of the mass distribution and the phase [19, 23]. It can produce circles in the Argand plot, the origin of which is the Regge phase factor $\exp[-i\frac{1}{2}\pi\alpha(t_R)]$.

Figure 2: Deck background production in $\eta\pi$.



It is also important to note that rescattering of the lighter particle from the dissociation of the incident beam particle is not a prerequisite, and indeed both can contribute [21]. We suggest that in our particular case the relevant processes are (from left to right in Figure 2)

1. $\pi \rightarrow b_1\omega$, $\omega p \rightarrow \pi p$ giving a $b_1\pi$ final state.
2. $\pi \rightarrow \pi\rho$, $\rho p \rightarrow \eta p$ giving a $\eta\pi$ final state.
3. $\pi \rightarrow \rho\pi$, $\pi p \rightarrow \pi p$ and $\rho p \rightarrow \rho p$ giving a $\pi\rho$ final state.

For each of these processes the rescattering will be predominantly via ρ (natural parity) exchange to give the required parity in the final state. Obviously process (ii) produces a final $\eta\pi$ state directly, but for (i) and (iii) the $b_1\pi$ and $\rho\pi$ final states are required to rescatter into $\eta\pi$ (for which the doorway calculation provides an explicit mechanism).

Unfortunately only the πp cross section can be obtained with any reliability. The others can be estimated with varying degrees of uncertainty from:

1. $\pi\rho \rightarrow b_1\pi$: data on $\pi^0 p \rightarrow \omega n$, which can be inverted to give $\omega p \rightarrow \pi^0 p$.
2. $\pi\rho \rightarrow \eta\pi$: data on $\gamma p \rightarrow \eta p$, which by assuming vector meson dominance can give $\rho p \rightarrow \eta p$.
3. $\pi\rho \rightarrow \rho\pi$: data on $\pi^- p \rightarrow \pi^0 n$ and on $\pi^\pm p \rightarrow \pi^\pm p$; data on $\gamma p \rightarrow \rho p$ and vector meson dominance.

In view of the uncertainties in the underlying reactions, the lack of an explicit value for the $J^{PC} = 1^{-+}$ $\eta\pi$ cross section in the E852 experiment, and the impossibility of a precise

evaluation of the rescattering into the $\eta\pi$ channel from $\rho\pi$ and $b_1\pi$, we have not attempted a complete Deck-type calculation. We concentrate rather on the mass-dependence which it generates. The characteristic mass-dependence is a peak just above the threshold. Thus there are three peaks from our proposed mechanism: a sharp peak just above the $\eta\pi$ threshold; a broader one at about 1.2 GeV from the $\rho\pi$ channel; and a very broad one at about 1.4 GeV from the $b_1\pi$ channel. The first of these is effectively removed by experimental cuts, but the net effect of the two latter is to produce a broad peak in the $\eta\pi$ channel. Thus invoking this mechanism does provide an explanation of the larger width of the $\eta\pi$ peak at 1.4 GeV in the E852 data compared to that of the $\rho\pi$ peak at 1.6 GeV. Because of the resonance-like nature of Deck amplitudes it is also possible in principle to simulate the phase variation observed. However as there are Deck amplitudes and the 1.6 GeV resonance, presumably produced directly, it is necessary to allow for interference between them. We use the K-matrix formalism to calculate this, and also to demonstrate that the Deck mechanism is essential to produce the 1.4 GeV peak.

3.3 K-matrix with P-vector formalism

It is straightforward to demonstrate that within the K-matrix formalism it is impossible to understand the $\eta\pi$ peak at 1.4 GeV as due to a 1.6 GeV state if only resonant decays to $\eta\pi$, $\rho\pi$ and $b_1\pi$ are allowed despite the strong threshold effects in the two latter channels³. We find that for a $b_1\pi$ width of ≈ 200 MeV and $\eta\pi$ and $\rho\pi$ widths in the region 1 – 200 MeV there is no shift of the peak. However, when a non-resonant $\eta\pi$ P-wave is introduced, the interference between this and the 1.6 GeV state can appear as a 1.4 GeV peak in $\eta\pi$.

We have seen that the non-resonant $\eta\pi$ wave can have significant presence at the $b_1\pi$ or $f_1\pi$ threshold (called the “P+S” threshold), e.g. 1.368 GeV for $b_1\pi$, because of the substantial “width” generated by the Deck mechanism. Since the hybrid is believed to couple strongly to “P+S” states due to selection rules [13, 15], the interference effectively shifts the peak in $\eta\pi$ down from 1.6 GeV to 1.4 GeV. It is not necessary for the 1.6 GeV resonance to have a strong $\eta\pi$ decay. It is significant that the E852 experiment finds $\hat{\rho}$ at $1370 \pm 16_{-30}^{+50}$ MeV, near the $b_1\pi$ threshold, but not at 1.6 GeV. It is possible for a state to peak near the threshold of the channel to which it has a strong coupling, assuming that the (weak)

³The use of $b_1\pi$ is not critical here: any channel with a threshold near 1.4 GeV will suffice.

channel in which it is observed has a significant non-resonant origin.

We follow the K-matrix formalism in the P-vector approach as outlined in [24, 25]. We assume there to be a $\hat{\rho}$ with $m_{\hat{\rho}} = 1.6$ GeV as motivated by the structure observed in $\rho\pi$ [3]. The problem is simplified to the case where there is decay to two observed channels i.e $\eta\pi$ and $\rho\pi$, and one unobserved $P + S$ channel. These channels are denoted 1, 2 and 3 respectively. The production amplitudes and the amplitude after final-state interactions are grouped together in the 3-dimensional P- and F-vectors respectively. In order to preserve unitarity [24] we assume a real and symmetric 3×3 K-matrix. The amplitudes after final-state interactions and production are related by [24]

$$F = (I - iK)^{-1}P \quad (11)$$

We define the widths as

$$\Gamma_i = \gamma_i^2 \Gamma_{\hat{\rho}} \frac{B^2(q_i)}{B^2(q_i^{\hat{\rho}})} \rho(q_i) \quad i = 1, 2 \quad (12)$$

$$\Gamma_3 = \gamma_3^2 \Gamma_{\hat{\rho}} \rho(q_3) \quad (13)$$

where q_i is the breakup momentum in channel i from a state of effective mass w , and $q_i^{\hat{\rho}}$ is the breakup momentum in channel i from a state of effective mass $m_{\hat{\rho}}$. The kinematics is taken care of by use of the phase space factor

$$\rho(q) = \frac{2q}{w} \quad (14)$$

and the P-wave angular momentum barrier factor

$$B^2(q) = \frac{(q/q_R)^2}{1 + (q/q_R)^2} \quad (15)$$

where the range of the interaction is $q_R = 1$ fm = 0.1973 GeV.

We assume the experimental width in $\rho\pi$ of $\Gamma_{\hat{\rho}} = 168$ MeV [3] to be the total width of the state⁴. We adopt the flux-tube model of Isgur and Paton [10] and use the $\rho\pi$ and $b_1\pi$

⁴It is found that our results in Fig. 3 are very similar even for a width of 250 MeV.

widths which it predicts for a hybrid of mass 1.6 GeV. Since the model predicts that the branching ratio of a hybrid to $b_1\pi$ is 59 – 74 % and to $f_1\pi$ is 12 – 16 % [17], we obtain the $P + S$ -wave width to be 120 – 150 MeV. Analysis of the data shows that the $\rho\pi$ branching ratio of $\hat{\rho}(1600)$ is 20 ± 2 % [6], corresponding to a $\rho\pi$ width of 30 – 37 MeV. This is consistent with flux-tube model predictions of 9 – 22 % [17]. For the simulation we use a $b_1\pi$ width of 120 MeV, a $\rho\pi$ width of 34 MeV, and an $\eta\pi$ width of 14 MeV, well within the limits set by the doorway calculation. We neglect other predicted modes of decay since we restrict our analysis to three channels.

The K-matrix elements are

$$K_{ij} = \frac{m_{\hat{\rho}}\sqrt{\Gamma_i\Gamma_j}}{m_{\hat{\rho}}^2 - w^2} + c_{ij} \quad (16)$$

where c_{ij} includes the possibility of an unknown background.

In the simulation we assume that the Deck terms can be treated as conventional resonances. This is not necessary, but is done to reduce the number of free parameters. We assume that the $\eta\pi$ Deck amplitude is produced predominantly via the $b_1\pi$ and $\rho\pi$ channels, and so is modelled as a resonance at a mass $m_{b_1} = 1.32$ GeV and a width $\Gamma_{b_1} = 300$ MeV. This width fits the E852 data at low $\eta\pi$ invariant masses (see Figure 3a). The $\rho\pi$ background is assumed to peak at a mass $m_{b_2} = 1.23$ GeV with a width $\Gamma_{b_2} = 400$ MeV, which when plotted as an invariant mass distribution effectively peaks at ~ 1.15 GeV, in agreement with detailed Deck calculations in the 1^{++} wave [19].

We incorporate the $\eta\pi$ and $\rho\pi$ Deck background by putting $c_{ij} = 0$ except for

$$c_{11} = \frac{m_{b_1}\Gamma_{b_1}}{m_{b_1}^2 - w^2} \quad c_{22} = \frac{m_{b_2}\Gamma_{b_2}}{m_{b_2}^2 - w^2} \quad (17)$$

The widths are defined analogously to Eq. 12 as

$$\Gamma_{bi} = \gamma_{bi}^2 \Gamma_{\hat{\rho}} \frac{B^2(q_i)}{B^2(q_i^b)} \rho(q_i) \quad i = 1, 2 \quad (18)$$

where q_i^b is the breakup momentum from a state of effective mass m_{bi} (for $i = 1, 2$).

The production amplitudes are given by

$$P_i = \frac{m_{\hat{\rho}} V_{\hat{\rho}} \sqrt{\Gamma_i \Gamma_{\hat{\rho}}}}{m_{\hat{\rho}}^2 - w^2} + c_i \quad (19)$$

where the (dimensionless) complex number $V_{\hat{\rho}}$ measures the strength of the production of $\hat{\rho}$. We take $c_3 = 0$ and

$$c_1 = \frac{m_{b_1} V_{b_1} \sqrt{\Gamma_{b_1} \Gamma_{\hat{\rho}}}}{m_{b_1}^2 - w^2} \quad c_2 = \frac{m_{b_2} V_{b_2} \sqrt{\Gamma_{b_2} \Gamma_{\hat{\rho}}}}{m_{b_2}^2 - w^2} \quad (20)$$

where the complex numbers V_{b_i} gives the production strengths of the Deck background in channel i .

The results of this fit are shown in Fig. 3 and clearly provide a good description of the $\eta\pi$ data [1, 25].

We briefly discuss the results. Fig. 3a indicates a steep rise for low invariant $\eta\pi$ masses, and a slow fall for large $\eta\pi$ masses. This naturally occurs because of the presence of the resonance at 1.6 GeV in the high mass region, which shows as a shoulder in our fit. Figure 3b reproduces the experimental slope and phase change in $\eta\pi$ [25]. One might find this unsurprising, since the background changes phase like a resonance. However, we have confirmed, by assuming a background that has constant phase as a function of $\eta\pi$ invariant mass, that the experimental phase shift is still reproduced. The experimental phase shift is hence induced by the resonance at 1.6 GeV.

Our fit to E852 $\eta\pi$ and $\rho\pi$ data (with a prediction for the $b_1\pi$ data) requires 12 independent parameters (see the caption of Figure 3).

Without the inclusion of a dominant $P+S$ -wave channel ⁵ the $\eta\pi$ event shape clearly shows two peaks, one at 1.3 GeV and one at 1.6 GeV, which is not consistent with the data [1]. The phase motion is also more pronounced in the region between the two peaks than that suggested by the data [25]. The rôle of the dominant $P+S$ -channel is thus that at invariant masses between the two peaks, the formalism allows coupling of the strong $P+S$ channel to $\eta\pi$, so that the $\eta\pi$ appears stronger than it would otherwise, interpolating between the peaks at 1.3 and 1.6 GeV, consistent with the data [1]. A dominant $P+S$ decay of the $\hat{\rho}$ is hence suggested by the data.

⁵The $b_1\pi$ coupling of the resonance is set to zero, with the $\eta\pi$ and $\rho\pi$ couplings the same as before.

4 Discussion

We have argued that on the basis of our current understanding of meson masses it is implausible to interpret the 1.4 GeV peak seen in the $J^{PC} = 1^{-+} \eta\pi$ channel by the BNL E852 experiment as evidence for an exotic resonance at that mass. We acknowledge that this is not a proof of non-existence and note the Crystal Barrel claim for the presence of a similar state at $1400 \pm 20 \pm 20$ MeV in the reaction $p\bar{p} \rightarrow \eta\pi^+\pi^-$. However this is not seen as a peak and is inferred from the interference pattern on the Dalitz plot. It has not been observed in other channels in $p\bar{p}$ annihilation at this mass, which is required for confirmation. So at present we believe that the balance of probability is that the structure does not reflect a real resonance.

Given this view, it is then necessary to explain the data and in particular the clear peak and phase variation seen by the E852 experiment. Additionally the observation of the peak only in the $\eta\pi$ channel, which is severely suppressed by symmetrization selection rules, requires justification. We have dealt with these two questions in reverse order. We first demonstrate that final-state interactions can generate a sizable $\eta\pi$ decay. We believe that this result by itself is of considerable significance and is of wider relevance. We then suggest that the E852 $\eta\pi$ peak is due to the interference of a Deck-type background with a hybrid resonance of higher mass, for which the $\hat{\rho}$ at 1.6 GeV is an obvious candidate. This mechanism also provides the natural parity exchange for the former which is observed experimentally. The parametrization of the Deck background is found not to be critical.

A key feature in our scenario is the presence of the large “ $P + S$ ” amplitude which drives the mechanism. This should be observable both as a decay of the 1.6 GeV state and as a lower-mass enhancement due to the Deck mechanism. Depending on the relative strength of these two terms the resulting mass distribution could be considerably distorted from a conventional Breit-Wigner shape as the Deck peak is broad and the interference could be appreciably greater than in the $\rho\pi$ channel.

Acknowledgements

Helpful discussions with S.-U. Chung and D.P. Weygand are acknowledged. The work of A.D. was supported by the University of Manchester and an invitation from TJNAF. P.R.P.

acknowledges a Lindemann Fellowship from the English Speaking Union.

A Appendix A: Decay of orbitally excited hybrid

We detail here the flux-tube model calculation for the decay of an orbitally excited hybrid to $P + S$ -wave mesons. The normalized wave functions of the P-wave and S-wave mesons are just S.H.O. wave functions with the same inverse radius β [13], and are respectively

$$2\sqrt{\frac{2}{3}} \frac{\beta^{5/2}}{\pi^{1/4}} r Y_{1ML}(\hat{\mathbf{r}}) \exp -\frac{1}{2}\beta^2 r^2 \quad \frac{\beta^{3/2}}{\pi^{3/4}} \exp -\frac{1}{2}\beta^2 r^2 \quad (21)$$

The normalized wave function of the orbitally excited hybrid is taken to be

$$\mathcal{N}_{\hat{\rho}} r^{\delta} \mathcal{D}_{M_L^{\hat{\rho}} \Lambda}^L(\phi, \theta, -\phi) \exp -\frac{1}{2}\beta_{\hat{\rho}}^2 r^2 \quad \mathcal{N}_{\hat{\rho}} = \sqrt{\frac{(2L+1)\beta_{\hat{\rho}}^{3+2\delta}}{2\pi\Gamma(\frac{3}{2}+\delta)}} \quad (22)$$

where the Wigner D-function $\mathcal{D}_{M_L^{\hat{\rho}} \Lambda}^L$ guarantees that the state has total orbital angular momentum $L = 2$, the first orbital excitation above the ground state with total orbital angular momentum 1, $M_L^{\hat{\rho}}$ is the total orbital angular momentum projection, and $\Lambda = \pm 1$ is the angular momentum of the flux-tube around the $Q\bar{Q}$ -axis [10]. The inverse radius $\beta_{\hat{\rho}}$ characterizes the size of the wave function and Γ is the Gamma-function. The radial dependence is chosen to be proportional to r^{δ} , where δ is chosen such radial Schrödinger equation [10] in the limit $r \rightarrow 0$, which leads to the condition $\delta(\delta+1) = L(L+1) - \Lambda^2$ [13], implying that $\delta = 1.79$ for $L = 2$. The lowest orbitally excited hybrid has the $Q\bar{Q}$ in spin 1, just like the ground state hybrid.

The relevant overlap can be obtained by inserting the spacial wave functions into the decay matrix element and performing the integration over the quark-antiquark pair creation position [13, 10]

$$\begin{aligned} \mathcal{M}_{M_L^{\hat{\rho}} M_L} = \text{flavour} & \frac{0.62 \gamma_0}{(1 + \frac{0.1}{\beta^2})^2} \frac{\sqrt{2}}{\beta} \mathcal{N}_{\hat{\rho}} \int_0^{2\pi} d\phi \int_0^{\pi} \sin\theta d\theta \int_0^{\infty} r^2 dr r^{\delta} (-i\beta^2 \mathbf{r} + \mathbf{p}) \cdot \mathbf{e}_{M_L^{\hat{\rho}} - M_L}^* \\ & \times \mathcal{D}_{M_L^{\hat{\rho}} 1}^2(\phi, \theta, -\phi) \mathcal{D}_{M_L 1}^{1*}(\phi, \theta, -\phi) \exp \frac{i}{2} \mathbf{p} \cdot \mathbf{r} \exp -\frac{1}{4} r^2 (2\beta_{\hat{\rho}}^2 + \beta^2) \end{aligned} \quad (23)$$

where \mathbf{p} is the momentum of the outgoing mesons in the rest frame of the hybrid and \mathbf{e} a spherical basis vector. Notice that the pair creation constant γ_0 of the 3P_0 model enters

explicitly in Eq. 23. This is because the flux-tube model, within the assumptions made for the wave functions, gives a prediction for the couplings of a hybrid in terms of couplings for mesons in the 3P_0 model [13] (the constants 0.62 and 0.1 in Eq. 6 are derived from flux-tube dynamics). We take $\gamma_0 = 0.39$ [13, 26, 10]. The integral in Eq. 23 is performed numerically.

We can write the decay amplitudes in terms of the amplitudes in Eq. 23 as follows, following ref. [13]. For $b_1\pi$ (“flavour” = 2):

$$\begin{aligned} \text{S-wave amplitude} &= -\frac{1}{\sqrt{15}}\Im (\sqrt{6}\mathcal{M}_{21} + \sqrt{3}\mathcal{M}_{11} + \mathcal{M}_{01} + \sqrt{3}\mathcal{M}_{10} + \mathcal{M}_{00}) \\ \text{D-wave amplitude} &= -\frac{1}{\sqrt{30}}\Im (\sqrt{6}\mathcal{M}_{21} + \sqrt{3}\mathcal{M}_{11} + \mathcal{M}_{01} - 2\sqrt{3}\mathcal{M}_{10} - 2\mathcal{M}_{00}) \end{aligned} \quad (24)$$

where \Im selects the imaginary part of the amplitude. For $f_1\pi$ and $a_1\eta$ (“flavour” = $\sqrt{2}$ and 1 respectively):

$$\begin{aligned} \text{S-wave amplitude} &= \frac{1}{\sqrt{30}}\Im (\sqrt{6}\mathcal{M}_{21} + \sqrt{3}\mathcal{M}_{11} + \mathcal{M}_{01} + \sqrt{3}\mathcal{M}_{10} + \mathcal{M}_{00}) \\ \text{D-wave amplitude} &= \frac{1}{2\sqrt{15}}\Im (\sqrt{6}\mathcal{M}_{21} - 2\sqrt{3}\mathcal{M}_{11} - 5\mathcal{M}_{01} + \sqrt{3}\mathcal{M}_{10} + \mathcal{M}_{00}) \end{aligned} \quad (25)$$

The $K_1(1270)$ is regarded as $\cos \tilde{\theta} |^1P_1\rangle + \sin \tilde{\theta} |^3P_1\rangle$ and $K_1(1400)$ the orthogonal partner, with $\tilde{\theta} = -34^\circ$ [13, 10]. 1P_1 and 3P_1 are the P-wave mesons with $Q\bar{Q}$ combinations of the decay amplitudes to the 1P_1 meson (Eq. 24) and 3P_1 meson (Eq. 25). For $K_1(1270)K$ and $K_1(1400)K$ “flavour” = $\sqrt{2}$.

For $f_2\pi$, $a_2\eta$ and $K_2^*(1430)K$ (“flavour” = $\sqrt{2}$, 1 and $\sqrt{2}$ respectively):

$$\text{D-wave amplitude} = \frac{1}{2\sqrt{5}}\Im (\sqrt{6}\mathcal{M}_{21} - \mathcal{M}_{01} - \sqrt{3}\mathcal{M}_{10} - \mathcal{M}_{00}) \quad (26)$$

The decay amplitudes in Eqs. 24 - 26 are then used to calculate widths according to the phase space conventions of Eq. 6 of ref. [13].

B Appendix B: Doorway calculation constants

B.1 $g_{\hat{\rho}b_1\pi}^S$ and $g_{\hat{\rho}b_1\pi}^D$

These couplings cannot be obtained from experiment, as there is currently no published data on the $\hat{\rho}^+$ coupling to $b_1^+\pi^0$. We have calculated $g_{\hat{\rho}b_1\pi}^S$ and $g_{\hat{\rho}b_1\pi}^D$ in the non-relativistic flux-tube model of Isgur and Paton, following the conventions and methods of ref. [13] (except that we assume the relativistic phase space convention [26]). The wave functions of the mesons and the hybrid are given respectively by Eqns. 21 and 22 (with $L = 1$). We find that

$$\begin{pmatrix} g_{\hat{\rho}b_1\pi}^S \\ g_{\hat{\rho}b_1\pi}^D \end{pmatrix} = -\sqrt{4m_{\hat{\rho}}E_{b_1}E_{\pi^0}} \begin{pmatrix} -2\varpi_1 + 3\varpi_2 + \varpi_3 \\ \frac{m_{b_1}}{m_{\hat{\rho}}p^2}(3(\varpi_2 + \varpi_3) + (\frac{E_{b_1}}{m_{b_1}} - 1)(-2\varpi_1 + 3\varpi_2 + \varpi_3)) \end{pmatrix} \quad (27)$$

where

$$\begin{pmatrix} \varpi_1 \\ \varpi_2 \\ \varpi_3 \end{pmatrix} = \frac{0.62 \gamma_0}{(1 + \frac{0.1}{\beta^2})^2} \frac{2}{\beta} \sqrt{\frac{\pi\beta_{\hat{\rho}}^{3+2\delta}}{3\Gamma(\frac{3}{2} + \delta)}} \int_0^\infty dr r^{2+\delta} \exp(-\frac{r^2}{4}(2\beta_{\hat{\rho}}^2 + \beta^2)) \begin{pmatrix} \beta^2 r j_0(\frac{pr}{2}) \\ p j_1(\frac{pr}{2}) \\ \beta^2 j_2(\frac{pr}{2}) \end{pmatrix} \quad (28)$$

where j_i and Γ refers to the spherical Bessel and Gamma functions respectively. We use $\gamma_0 = 0.53$ which reproduces conventional meson decay phenomenology for relativistic phase space [26]. In Eq. 27, β refers to the inverse radius of the b_1^+ or π^0 , the parameter that enters in the S.H.O. wave function. Similarly, $\beta_{\hat{\rho}}$ is the inverse radius of $\hat{\rho}^+$.

Setting $\delta = 1$, $\beta_{\hat{\rho}} = 0.27$ GeV and $\beta = 0.36$ GeV, yields

$$g_{\hat{\rho}b_1\pi}^S = 3.0 \text{ GeV} \quad g_{\hat{\rho}b_1\pi}^D = -8.2 \text{ GeV}^{-1} \quad (29)$$

We chose a value of γ_0 towards the upper end of the range in the literature. In calculations of excited mesons, values of γ_0 as low as .4 have been used [27]. The values for $g_{\hat{\rho}b_1\pi}^S$ and $g_{\hat{\rho}b_1\pi}^D$ can hence be only .4/.53 of the values quoted.

B.2 $g_{b_1\rho\eta}^S$ and $g_{b_1\rho\eta}^D$

Although the b_1^+ coupling to $\rho^+\eta$ is not known experimentally [28], its coupling to $\omega\pi^+$ is well known [28], and can be used to obtain the $\rho^+\eta$ coupling. We first derive the $\omega\pi$

coupling by assuming that 100% of the decays of b_1^+ is to $\omega\pi^+$ and using the experimentally measured D–wave to S–wave amplitude ratio.

The amplitude for $b_1^+ \rightarrow \omega\pi^+$ can be written as

$$\mathcal{M}_{b_1 \rightarrow \omega\pi} = \epsilon_\mu^{b_1} \epsilon_\nu^{\omega*} (g_{b_1\omega\pi}^S g^{\mu\nu} + g_{b_1\omega\pi}^D p_\omega^\mu p_{b_1}^\nu) \quad (30)$$

Using the Jacob–Wick formulae we write the S–wave and D–wave decay amplitudes as

$$\mathcal{M}_{b_1 \rightarrow \omega\pi}^S = \sqrt{\frac{4}{3}} \mathcal{M}_{b_1 \rightarrow \omega\pi}^{\epsilon=\uparrow} + \sqrt{\frac{1}{3}} \mathcal{M}_{b_1 \rightarrow \omega\pi}^{\epsilon=\rightarrow} = \frac{1}{\sqrt{3}} (-2g_{b_1\omega\pi}^S - \frac{E_\omega}{m_\omega} g_{b_1\omega\pi}^S + p_\omega^2 \frac{m_{b_1}}{m_\omega} g_{b_1\omega\pi}^D) \quad (31)$$

$$\mathcal{M}_{b_1 \rightarrow \omega\pi}^D = \sqrt{\frac{2}{3}} \mathcal{M}_{b_1 \rightarrow \omega\pi}^{\epsilon=\uparrow} - \sqrt{\frac{2}{3}} \mathcal{M}_{b_1 \rightarrow \omega\pi}^{\epsilon=\rightarrow} = \sqrt{\frac{2}{3}} ((\frac{E_\omega}{m_\omega} - 1) g_{b_1\omega\pi}^S - p_\omega^2 \frac{m_{b_1}}{m_\omega} g_{b_1\omega\pi}^D) \quad (32)$$

where all energies and momenta refer to the b_1^+ rest frame. Relating the S–wave and D–wave amplitudes to the corresponding widths in the usual way (analogous to Eq. 10), we finally obtain

$$\begin{pmatrix} g_{b_1\omega\pi}^S \\ g_{b_1\omega\pi}^D \end{pmatrix} = 2\sqrt{\frac{\pi}{p_\omega}} \sqrt{\frac{\Gamma_{total}}{1 + (\sqrt{\frac{\Gamma^D}{\Gamma^S}})^2}} \begin{pmatrix} m_{b_1}(\sqrt{2} + \sqrt{\frac{\Gamma^D}{\Gamma^S}}) \\ \frac{m_\omega}{p_\omega^2}(\sqrt{2}(\frac{E_\omega}{m_\omega} - 1) + (\frac{E_\omega}{m_\omega} + 2)\sqrt{\frac{\Gamma^D}{\Gamma^S}}) \end{pmatrix} \quad (33)$$

Using the experimental data $\Gamma_{total} = 142 \pm 8$ GeV and $\sqrt{\frac{\Gamma^D}{\Gamma^S}} = +0.29 \pm 0.04$ (where the sign is taken to mean that the D–wave and S–wave amplitudes have the same sign), we obtain can then deduce the coupling constants

$$g_{b_1\omega\pi}^S = 4.6 \pm 0.2 \text{ GeV} \quad g_{b_1\omega\pi}^D = 14.4 \pm 2.2 \text{ GeV}^{-1} \quad (34)$$

To obtain the b_1 coupling to $\rho^+\eta$, we note that (neglecting effects due to phase space), it should be related to the $\omega\pi^+$ coupling by a simple flavour factor. This is because the Lorentz structure of the two decays are identical. Assuming that the decomposition of the η which is motivated by experiment, i.e. $\eta = \frac{1}{\sqrt{2}}(\frac{1}{\sqrt{2}}(u\bar{u} + d\bar{d}) + s\bar{s})$, we have

$$g_{b_1\rho\eta}^S = \frac{1}{\sqrt{2}} g_{b_1\omega\pi}^S = 3.2 \pm 0.1 \text{ GeV} \quad g_{b_1\rho\eta}^D = \frac{1}{\sqrt{2}} g_{b_1\omega\pi}^D = 10.2 \pm 1.5 \text{ GeV}^{-1} \quad (35)$$

We have also performed a flux-tube (3P_0) model calculation to independently derive the coupling constants. For $\gamma_0 = 0.53$, $\beta = 0.4$ GeV we obtain

$$g_{b_1\rho\eta}^S = 3.4 \text{ GeV} \quad g_{b_1\rho\eta}^D = 10.6 \text{ GeV}^{-1} \quad (36)$$

The agreement (both in sign and magnitude) is clearly impressive, underlining the significant agreement of the 3P_0 model with experiment [26].

B.3 $g_{\rho\pi\pi}$

Here we assume that 100% of the decays of ρ^+ are to $\pi^+\pi^0$ [28]. We evaluate the amplitude Eq. 3 in the rest frame of ρ^+ and connect the amplitude to the width of 150.7 ± 0.6 MeV [28], according to the usual relation (analogous to Eq. 10) to obtain

$$g_{\rho\pi\pi} = 6.02 \pm 0.02 \quad (37)$$

References

- [1] D.R. Thompson *et al.* (E852 Collab.), *Phys. Rev. Lett.* **79** (1997) 1630.
- [2] A. Abele *et al.* (Crystal Barrel Collab.), *Phys. Lett.* **B423** (1998) 175; W. Dünnweber (Crystal Barrel Collab.), *Proc. of HADRON'97* (Upton, N.Y., August 1997), p. 309, eds. S.-U. Chung, H.J. Willutzki.
- [3] N.M. Cason (E852 Collab.), *Proc. of Intersections between Nuclear and Particle Physics*, p. 471 (Big Sky, Montana, May 1997), ed. T.W. Donnelly, American Institute of Physics; D.P. Weygand and A.I. Ostrovidov (E852 Collab.), *Proc. of HADRON '97* (Upton, N.Y., August 1997), p. 313, 263, eds. S.-U. Chung, H.J. Willutzki; A.I. Ostrovidov *et al.* (E852 Collab.), *in preparation*.
- [4] Yu.P. Gouz. *et al.* (VES Collab.), *Proc. of the 26th ICHEP* (Dallas, 1992), p. 572, ed. J.R. Sanford.
- [5] D. Ryabchikov (E852 Collab.), “Study of the reaction $\pi^-p \rightarrow \eta\pi^+\pi^-\pi^-p$ in E852 experiment”, *Proc. of HADRON'97* (Upton, N.Y., August 1997), p. 527, eds. S.-U. Chung,

- H.J. Willutzki; Yu.P. Gouz. *et al.* (VES Collab.), *Proc. of the 26th ICHEP* (Dallas, 1992), p. 572, ed. J.R. Sanford.
- [6] P.R. Page, *Phys. Lett.* **B415** (1997) 205.
- [7] T. Barnes, F.E. Close and E.S. Swanson, *Phys. Rev.* **D52** (1995) 5242.
- [8] C. Michael *et al.*, *Nucl. Phys.* **B347** (1990) 854; *Phys. Lett.* **B142** (1984) 291; *Phys. Lett.* **B129** (1983) 351; *Liverpool Univ. report LTH-286* (1992), *Proc. of the Workshop on QCD : 20 Years Later* (Aachen, 9–13 June 1992).
- [9] P.R. Page, *Phys. Lett.* **B401** (1997) 313; F. Iddir *et al.*, *Phys. Lett.* **B207** (1988) 325; H.J. Lipkin, *Phys. Lett.* **219** (1989) 99; S.F. Tuan, T. Ferbel, R.H. Dalitz, *Phys. Lett.* **B213** (1988) 537; S.F. Tuan, *Mod. Phys. Lett. A*, Vol.6, No.9 (1991) 789.
- [10] N. Isgur and J.E. Paton, *Phys. Rev.* **D31** (1985) 2910; R. Kokoski, N. Isgur, *Phys. Rev.* **D35** (1987) 907.
- [11] S. Collins (UKQCD Collab.), *Nucl. Phys. Proc. Suppl.* **63** (1998) 335.
- [12] I.I. Balitsky, D.I. Dyakonov, A.V. Yung, *Z. Phys.* **C33** (1986) 265.
- [13] F.E. Close, P.R. Page, *Nucl. Phys.* **B443** (1995) 233; *Phys. Rev.* **D52** (1995) 1706.
- [14] F. Iddir, S. Safir, O. Pène, hep-ph/9803470.
- [15] P.R. Page, *Phys. Lett.* **B402** (1997) 183.
- [16] J.I. Latorre *et al.*, *Z. Phys.* **C34** (1987) 347; S. Narison, “QCD spectral sum rules”, *Lecture Notes in Physics*, Vol. 26 (1989), p. 369; J. Govaerts, F. de Viron, *Phys. Rev. Lett.* **53** (1984) 2207.
- [17] P.R. Page, *Proc. of HADRON’97* (Upton, N.Y., August 1997), p. 121, eds. S.-U. Chung, H.J. Willutzki, hep-ph/9711241; P.R. Page, E.S. Swanson, A.P. Szczepaniak, *in preparation*.
- [18] M.P. Locher, Y. Lu and B.S. Zou, *Z.Phys.* **A347** (1994) 281.
- [19] G. Ascoli *et al.* *Phys. Rev.* **D8** (1973) 3894; *ibid.* **D9** (1974) 1963.
- [20] O. Gortchakov *et al.*, *Z.Phys.* **A353** (1996) 447.

- [21] L. Stodolsky, *Phys. Rev. Lett.* **18** (1967) 973.
- [22] V. Gribov, *Sov. J. Nucl. Phys.* **5** (1967) 138; M.R.O. Morrison, *Phys. Rev.* **165** (1968) 1699.
- [23] M.G. Bowler *et al.*, *Nucl. Phys.* **B97** (1975) 227; M.G. Bowler, *J. Phys.* **G5** (1979) 203.
- [24] I.J.R. Aitchison, *Nucl. Phys.* **A189** (1972) 417; S.-U. Chung *et al.*, *Ann. der Phys.* **4** (1995) 404.
- [25] S.-U. Chung, Private communication; *Proc. of Jefferson Lab / NCSU Workshop on Hybrids and Photoproduction Physics* (1997).
- [26] P. Geiger, E.S. Swanson, *Phys. Rev.* **D50** (1994) 6855.
- [27] T. Barnes, F.E. Close, P.R. Page, E.S. Swanson, *Phys. Rev.* **D55** (1997) 4157.
- [28] Particle Data Group, *Phys. Rev.* **D54** (1996) 1.

Figure 3: Results of the K-matrix analysis. (a) The events ($|F_1|^2$) in $\eta\pi$ as compared to experiment [1]; (b) The phase (of F_1) in $\eta\pi$ compared to experiment [25]. The invariant mass w is plotted on the horizontal axis in GeV. When the phase is plotted it is in radians, with the overall phase *ad hoc*. The parameters of the simulation are $m_{\hat{\rho}} = 1.6$ GeV, $\Gamma_{\hat{\rho}} = 168$ MeV [3], $\gamma_1 = 0.31$, $\gamma_2 = 0.52$, $\gamma_3 = 1.49$, $m_{b_1} = 1.32$ GeV, $m_{b_2} = 1.23$ GeV, $\gamma_{b_1} = 1.53$, $\gamma_{b_2} = 2.02$, $V_{b_1}/V_{\hat{\rho}} = 2.05e^{2.77i}$, $V_{b_2}/V_{b_1} = 0.35e^{1.6i}$. $V_{\hat{\rho}}$ sets the overall magnitude and phase, which is not shown. None of the ratios of production strengths should be regarded as physically significant, since the K-matrix formalism allows for the introduction of additional parameters in the modelling of the backgrounds, which would change the values of these ratios. The plots shown here are only weakly dependent on the $\rho\pi$ parameters γ_{b_2} and V_{b_2} . The parameters have been chosen to fit both the $\eta\pi$ data [1] and the preliminary $\rho\pi$ data [3]. Experiment has not been able to eliminate the possibility that the low mass peak in $\rho\pi$ is due to leakage from the a_1 . The background amplitude in $\rho\pi$ is being used as a means of parametrising all forms of background into the $\rho\pi$ channel, including leakage or Deck.

